Iodine-123-IBZM Dopamine D2 Receptor and Technetium-99m-HMPAO Brain Perfusion SPECT in the Evaluation of Patients with and Subjects at Risk for Huntington's Disease

Masanori Ichise, Hiroshi Toyama, Luis Fornazzari, James R. Ballinger and Joel C. Kirsh

Department of Nuclear Medicine, Mount Sinai Hospital and University of Toronto, Toronto, Ontario, Canada; Department of Radiology, Fujita Health University, Toyoake, Japan; Department of Neurology, Clarke Institute of Psychiatry, Toronto, Ontario, Canada; Department of Nuclear Medicine, Princess Margaret Hospital, Toronto, Ontario, Canada

Huntington's disease (HD) is pathologically characterized by neuronal loss and neuroreceptor alterations in the striatum, including a reduction in dopamine receptor density. We evaluated the clinical usefulness of ^{123}I-iodobenzamide (IBZM) D2 receptor SPECT imaging and ^{99m}Tc-hexamethylpropyleneamineoxime (HMPAO) brain perfusion SPECT imaging by studying four early symptomatic HD patients, 20 asymptomatic subjects at risk for HD and 22 controls. Striatal D2 receptor binding and perfusion were measured semiquantitatively by calculating striatum-to-frontal cortex IBZM and HMPAO uptake ratios, respectively. The control IBZM ratio (1.58 ± 0.06) declined with age at 1.5% per decade ($r = -0.58$, $p < 0.005$), whereas the HMPAO ratio (1.15 ± 0.05) did not. All four symptomatic patients had decreased IBZM ratios and three patients also had decreased HMPAO ratios. Five of 20 at-risk subjects had decreased IBZM ratios and two subjects also had decreased HMPAO ratios. Three of the five at-risk subjects showed subtle nonchoreic neurological abnormalities. Decreased striatal D2 receptor binding thus may be detected by IBZM-SPECT in the asymptomatic as well as symptomatic groups, and these changes were more marked than perfusion deficits detected by HMPAO-SPECT. IBZM-SPECT thus appears to be a promising method for early diagnosis and preclinical detection of HD.

J Nucl Med 1993; 34:1274–1281

Huntington's disease (HD) is an autosomal dominant and fatal neurodegenerative disorder characterized by the insidious development of chorea, psychiatric disturbances and dementia (*1*). Pathologically, HD is characterized by neuronal loss, primarily in the caudate and putamen (*2*). This is associated with complex neurotransmitter-receptor alterations (*3–7*), including a marked decrease in the number of dopaminergic receptors (*3,7*) and either normal or increased concentrations of dopamine in the striatum (*4,6*). Clinically, HD usually does not manifest itself until the third or fourth decade of life. Thus, early diagnosis or preferably presymptomatic detection is important for genetic counselling (*8*).

Structural neuroimaging with x-ray computed tomography (CT) or magnetic resonance imaging can detect caudate atrophy that results from striatal neuronal loss, usually in the late but not the early stage of HD (*9–11*). In the early stage, functional neuroimaging with positron emission tomography (PET) and single-photon emission computerized tomography (SPECT) can detect striatal hypometabolism and/or hypoperfusion (*11–15*). This reflects a reduction in either the function or number of striatal neurons without detectable tissue loss, and this process may begin in the presymptomatic stage (*11,13–18*). However, neither striatal hypometabolism nor hypoperfusion is specific for HD, which occurs in other movement disorders as well (*19,20*).

The dopaminergic system has been implicated in the pathophysiology of the chorea seen in HD (*3,4,21*). Klawans et al. (*21*) were able to elicit choreiform movements in some asymptomatic subjects at risk for HD after administration of L-dopa. This suggests that the striatal dopaminergic receptor density may be decreased early in the course of the disease.

Techniques for in vivo measurements of neuroreceptor binding are now available. Leenders et al. (*22*) and Hagglund et al. (*23*) have demonstrated decreased D2 receptor binding in a small number of HD patients using ^{11}C-N-methylspiperone (NMSP) and PET. As new neuroreceptor radioligands become available, "gold standard" PET techniques will undoubtedly be utilized more often (*20*). However, due to its high cost and complexity, PET is currently available only at a relatively small number of research centers. In contrast, SPECT is widely available and more suited for practical clinical situations. Recently, ^{123}I-3-iodo-6-methoxybenzamide (IBZM) has been introduced as a D2 receptor imaging agent for use with SPECT (*24,25*)

Received Aug. 25, 1992; revision accepted Mar. 18, 1993.

For correspondence or reprints contact: Masanori Ichise, MD, FRCPC, Room 635, Nuclear Medicine, Radiological Sciences, Mount Sinai Hospital, 600 University Ave., Toronto, Ontario, Canada M5G 1X5.

and preliminary clinical studies with IBZM-SPECT in disorders of the dopaminergic system appear promising (*26,27*).

The purpose of the present study is to evaluate the clinical usefulness of IBZM D2 receptor SPECT imaging and ^{99m}Tc-hexamethylpropyleneamineoxime (HMPAO) brain perfusion SPECT imaging in early symptomatic HD patients and asymptomatic subjects at risk for HD.

MATERIALS AND METHODS

Subjects

A total of 24 case subjects, consisting of 4 early symptomatic HD patients (all males, mean age 45.2 ± 14.4 yr, disease duration 18 ± 6 mo) and 20 asymptomatic subjects at risk for HD (11 males, 9 females, mean age 31.5 ± 10.7 yr) and 22 normal control subjects (15 males, 7 females, mean age 39.7 ± 14.7 yr) participated in the study. These case subjects were selected from six families, including four families with a clear multigeneration family history of HD and the remaining two families with autopsy confirmation of HD in first degree family members. They received close follow-up by a neurologist (L.F.) for several years prior to the study. They were free of medication for at least 4 wk before participation in the study and none were on neuroleptic therapy. All symptomatic patients had adult onset chorea. All at-risk subjects were free of chorea. The control subjects consisted of healthy volunteers with no neuropsychiatric abnormalities or family history of movement disorders and were free of any drugs. The project was granted ethical approval by the Human Subjects Review Committee of the University of Toronto.

Neurological Examination

All case subjects were given a detailed neurological examination by a neurologist (L.F.) prior to the imaging studies. Functional capacity was assessed according to the method of Shoulson and Fahn (S&F) (*28*). The maximum score of 13 represents normal functioning. Involuntary movements were graded using the Marsden and Quinn's chorea scale (M&Q) (*29*). The range was 0–24, with the minimum score of 0 indicating no involuntary movements. The mini-mental state examination (MMS) (*30*) was also performed. The maximum score of 30 indicates normal mental status.

Preparation of IBZM

IBZM was labeled by a kit procedure developed by Kung et al. (*31*). In 15 preparations, the radiochemical yield was 49% ± 5% and the radiochemical purity was 94% ± 3%. Retrospective sterility testing was negative.

SPECT Imaging and Data Analysis

After informed consent was obtained, all subjects underwent HMPAO and then IBZM imaging 2 to 7 days apart. For HMPAO imaging, 20 mCi (740 MBq) of HMPAO, and for IBZM imaging, 5 mCi (185 MBq) of IBZM were injected intravenously in a quiet room with the subject's eyes open. Potassium iodide (Lugol's solution) was given prior to and for 3 days after the IBZM study.

SPECT imaging was performed using a truncated single-head rotating gamma camera interfaced to a dedicated computer (Elscint 409 ECT). For HMPAO-SPECT, sixty 25-sec images were obtained 30 min postinjection through a 360° circular orbit using a low-energy, high-resolution, parallel-hole collimator. IBZM-SPECT imaging timing was determined from in vivo kinetic data reported by Brücke et al. (*26*) and our previous data (*32*), which showed that specific striatal IBZM binding was in an apparent steady-state from 60 to 120 min post-IBZM injection. Thus, sixty 36-sec images were obtained 60 min postinjection through a 360° circular orbit using a low-energy, medium-resolution and medium sensitivity collimator. SPECT data were acquired in a 64 × 64 matrix. The radius of rotation was 14 cm or less. A Jaszczak phantom (model 7000, Data Spectrum Corporation) and capillary ^{99m}Tc and ^{123}I line sources were used and the FWHMs of the system equipped with collimators for HMPAO and IBZM imaging were 14 and 15 mm, respectively, at the center of the field of view with a rotation radius of 12 cm.

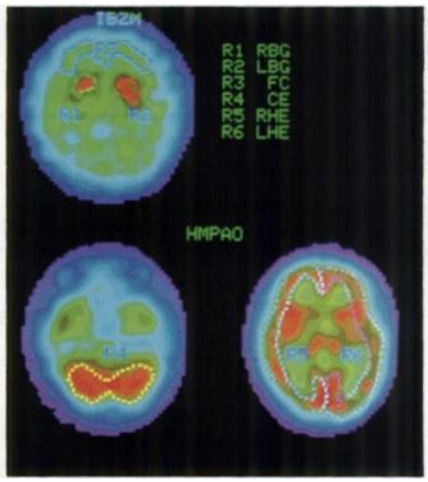

FIGURE 1. One transaxial IBZM and two HMPAO images with ROIs. RBG = right basal ganglia; LBG = left basal ganglia; FC = frontal cortex; CE = cerebellum; RHE = right cerebral cortical hemisphere; LHE = left cerebral cortical hemisphere.

One pixel-thick (4 mm) transaxial slices from the vertex of the brain to the level of the canthomeatal (CM) line were reconstructed using a modified Hanning backprojection filter. These were parallel to the CM line as determined from a preliminary lateral planar image with external radioactive markers identifying this line. The first order Chang method of attenuation correction (0.12 cm^{-1}) was employed (*33*).

By using our previously described stereotaxic technique (*34*), these transaxial images were standardized to yield a constant number of nine slices (~1.3 cm thick per slice) for all SPECT studies. For region of interest (ROI) placement on these nine slices, one slice was selected in which the basal ganglia were best visualized for each SPECT study and another slice in which the mid-cerebellar hemispheres were best visualized for each HMPAO study. ROIs were then drawn on these slices by outlining areas corresponding to the right and left basal ganglia (BG) and frontal cortex (FC) for both IBZM and HMPAO studies, and the right and left cerebral cortical hemispheres (HE) and cerebellum (CE) for all HMPAO studies (Fig. 1). ROI placement depended on visual identification of anatomical regions aided by the Talairach's stereotaxic brain atlas (*34,35*). The areas of these ROIs were: BG = 4.6 cm^2, FC = 17 cm^2, CE = 23 cm^2, and HE = 38 cm^2. The area of each ROI was kept the same for all subjects. All ROIs were drawn and applied by the same investigator (H.T.) to reduce interobserver variation. The investigator was blinded to any specific clinical information except whether the subject belonged to the normal control or case group.

Striatal D2 receptor binding was measured semiquantitatively by calculating IBZM BG-to-FC ratios. To assess relative striatal perfusion, HMPAO BG-to-FC, BG-to-CE and BG-to-HE ratios were calculated. In addition, relative frontal lobe perfusion was assessed by calculating HMPAO FC-to-CE ratios. All ratios were expressed as mean pixel count ratios.

TABLE 1
IBZM and HMPAO Ratios (mean ± 1 s.d.) and Comparison of Symptomatic and at Risk Groups with Normal Control Group

Group	IBZM BG-to-FC	HMPAO BG-to-FC	HMPAO BG-to-CE	HMPAO BG-to-HE	HMPAO FC-to-CE
Normals (n = 22)	1.58 ± 0.06	1.15 ± 0.05	1.01 ± 0.06	1.09 ± 0.06	0.88 ± 0.07
Symptomatic (n = 4)	1.29* ± 0.05	1.04* ± 0.01	0.97* ± 0.01	1.03* ± 0.02	0.93 ± 0.02
t-test	p < 0.00001	p < 0.00001	p < 0.01	p < 0.05	ns
At risk (n = 20)	1.55 ± 0.11	1.14 ± 0.06	0.99 ± 0.08	1.07 ± 0.05	0.87 ± 0.06
t-test	ns	ns	ns	ns	ns

*Decreased compared with the normal mean.
ns = no significant difference.

X-ray CT

Since no significant reduction in the size of the caudate nucleus was expected in our case subjects (*11–17,36*), CT was not included in the initial protocol. However, CT scans were obtained later in three symptomatic subjects and in five at-risk subjects. Based on the measurements made on a standard 10-mm transaxial slice, the ratio between the maximum bifrontal diameter and minimum bicaudate diameter was calculated and compared with those obtained by others (*9,36,37*).

Genetic Risk Calculation

The percentage of the subjects in the at-risk group that should on probability grounds have the HD gene was calculated based on their age at the time of the study and the sex of the affected parent. Calculations were made according to the methods previously described (*8,38*), which used population data on 999 HD-affected individuals.

Statistical Analysis

Two-tailed Student's t-tests for unpaired samples were used to compare groups. Statistical significance was defined as $p < 0.05$. Linear regression analysis was used to test for significant effect of age on IBZM and HMPAO ratios in the normal control group. If the test was significant, 95% confidence limits as well as 95% prediction limits for new values on the regression line at each age were calculated. In the case group, age-dependent 95% prediction limits were used to define normal values if regression analysis was significant; otherwise any values more than 2 s.d. below or above the normal mean were considered abnormal.

RESULTS

Total counts per SPECT study ranged from 3 to 7 million counts for HMPAO and from 2 to 5 million counts for IBZM. All SPECT studies were technically adequate.

Normal Control Subjects

IBZM and HMPAO ratios expressed as mean ±1 s.d. are shown in Table 1. There was an age-dependence factor of the IBZM BG-to-FC ratio, which declined significantly with increasing age ($r = -0.58$, $p < 0.005$), at 1.5% per decade (Fig. 2). The 95% confidence limits on the regression line at ages 20, 40 and 60 were 1.63 ± 0.04, 1.58 ± 0.02 and 1.53 ± 0.04, respectively; the 95% prediction limits for a new value of the BG-to-FC ratio at these ages were 1.63 ± 0.12, 1.58 ± 0.11 and 1.53 ± 0.12, respectively. The difference between right and left striatal IBZM uptake ratios was within 4%. There was no significant decline in HMPAO ratios as a function of age.

Case Subjects

In the symptomatic group, both mean BG-to-FC-IBZM and striatal HMPAO ratios (BG-to-FC, BG-to-CE and BG-to-HE) were all significantly decreased when compared to the normal mean (Table 1). All four HD patients had IBZM BG-to-FC ratios below the 95% prediction limits at their respective ages and also more than 2 s.d. below the normal mean (Table 2 and Fig. 3). Three HD patients also had decreased HMPAO BG-to-FC ratios that were more than 2 s.d. below the normal mean (Table 2 and Fig. 3). No subject in this group had increased striatal HMPAO ratios.

In the at-risk group, although there were no significant differences between mean IBZM or HMPAO ratios in this group and the normal mean (Table 1), five subjects had decreased IBZM BG-to-FC ratios below 95% prediction limits at their respective ages, including four ratios that were more than 2 s.d. and one ratio more than 1 s.d. below the normal mean (Table 2 and Fig. 3). No subject in this group showed increased IBZM BG-to-FC ratios above 95% prediction limits at their respective ages. Two of the above five subjects with decreased IBZM ratios also had decreased striatal HMPAO ratios, in which the BG-to-FC ratio was decreased in both and the BG-to-CE ratio decreased in one of the two subjects (Table 2 and Fig. 3). The BG-to-FC and BG-to-CE HMPAO ratios in the remainder

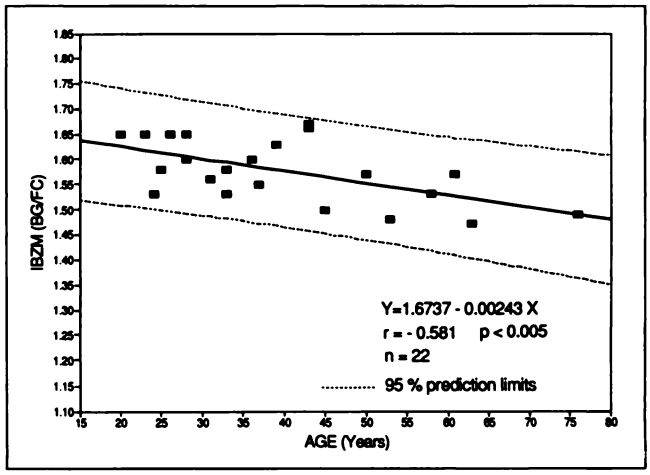

FIGURE 2. Relationship between IBZM BG-to-FC ratio and age in normal control subjects. The BG-to-FC ratio declined significantly with increasing age. Dotted lines indicate the age-dependent 95% prediction limits for a new value for this ratio.

TABLE 2
IBZM and HMPAO Ratios in Four Symptomatic HD Patients and 20 at Risk Subjects for HD

Case (Age)	IBZM BG-to-FC	HMPAO BG-to-FC	HMPAO BG-to-CE	HMPAO BG-to-HE	HMPAO FC-to-CE
Symptomatic					
1 (68)	1.36*	1.06	0.95	1.03	0.90
2 (28)	1.20*	1.04†	0.96	1.02	0.92
3 (43)	1.29*	1.02†	0.98	1.05	0.96
4 (42)	1.31*	1.03†	0.97	1.00	0.94
At Risk					
1 (64)	1.52	1.17	1.04	1.09	0.89
2 (42)	1.44*	1.22	1.11	1.17	0.91
3 (40)	1.34*	1.05†	1.05	1.03	1.00
4 (40)	1.56	1.14	1.05	1.02	0.92
5 (38)	1.50	1.06	0.91	1.01	0.87
6 (38)	1.56	1.15	0.93	1.05	0.81
7 (34)	1.32*	1.04†	0.86†	0.98	0.82
8 (34)	1.60	1.15	0.90	1.05	0.78
9 (32)	1.53	1.16	1.02	1.09	0.88
10 (31)	1.67	1.10	0.94	1.06	0.85
11 (30)	1.64	1.18	1.05	1.07	0.89
12 (30)	1.71	1.21	1.01	1.12	0.83
13 (29)	1.36*	1.08	0.90	1.04	0.83
14 (27)	1.59	1.23	1.07	1.05	0.87
15 (26)	1.72	1.15	0.94	1.03	0.82
16 (22)	1.61	1.23	0.99	1.16	0.81
17 (19)	1.51‡	1.13	1.11	1.09	0.99
18 (18)	1.55	1.12	1.00	1.15	0.89
19 (18)	1.58	1.10	1.09	1.08	0.99
20 (17)	1.70	1.10	0.92	1.06	0.84

*Below 95% prediction limits and greater than 2 s.d. below the normal mean.
†Greater than 2 s.d. below the normal mean.
‡Below 95% prediction limits and greater than 1 s.d. below the normal mean.

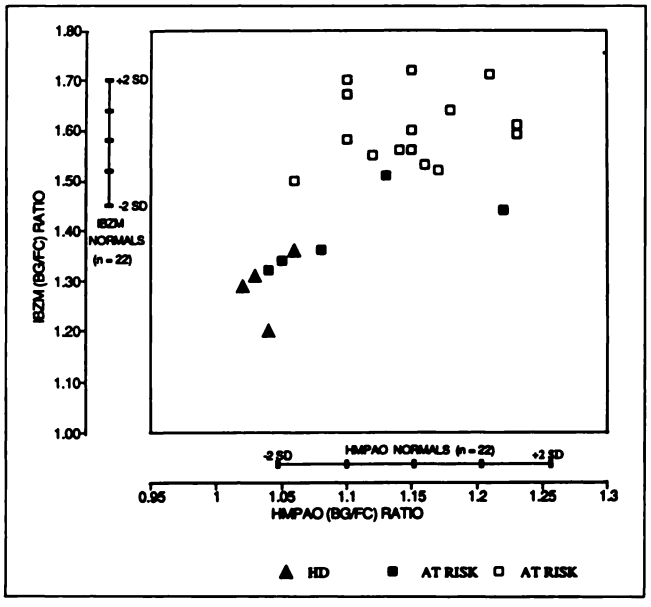

FIGURE 3. IBZM and HMPAO BG-to-FC ratios in symptomatic HD patients (n = 4) and subjects at risk for HD (n = 20). The range (mean ± 2 s.d.) of IBZM BG-to-FC ratios in the normal control group (n = 22) is shown on left along the ordinate and that for HMPAO BG-to-FC ratios at the bottom along the abscissa. Those subjects at risk for HD with IBZM ratios below 95% prediction limits (n = 5) are indicated by ☒ and those with IBZM ratios within 95% prediction limits (n = 15) by □.

of this group as well HMPAO BG-to-HE ratios in this entire group were all normal.

Right and left striatal IBZM uptakes were symmetrical within 4% in both symptomatic and at-risk groups. Relative frontal lobe perfusion as measured by HMPAO FC-to-CE ratios was normal in both groups. Representative IBZM and HMPAO images from a normal control subject, two at-risk subjects and one symptomatic patient are shown in Figure 4.

Neurological findings in the case subjects are summarized in Table 3. Combined SPECT imaging and neurological findings in the at-risk group are summarized in Table 4. Neurological findings indicated that all four symptomatic patients were considered to be in the early stages of HD (*28,39*). In the at-risk group, three of five subjects with decreased IBZM ratios, including one subject with a decreased HMPAO BG-to-FC ratio showed subtle motor abnormalities in all three (M&Q scores ranging from 1/24 to 2/24) and also a slight attention deficit in one (MMS score of 28/30). One subject with both normal IBZM and HMPAO ratios also showed subtle motor abnormalities (M&Q score of 1/24). These motor abnormalities consisted of occasional, noncharacteristic facial and/or limb "twitches." No abnormalities of eye movements, such as saccadic movements or impaired optokinetic nystagmus, were detected in these subjects. These subtle but nonchoreic mo-

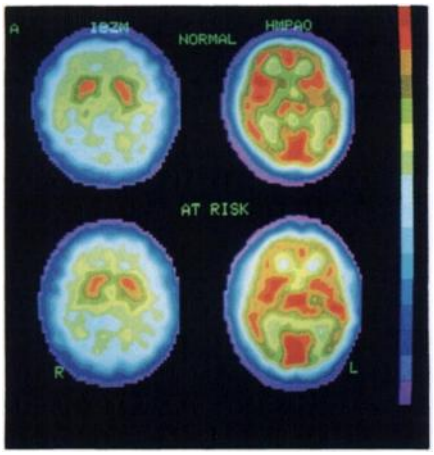

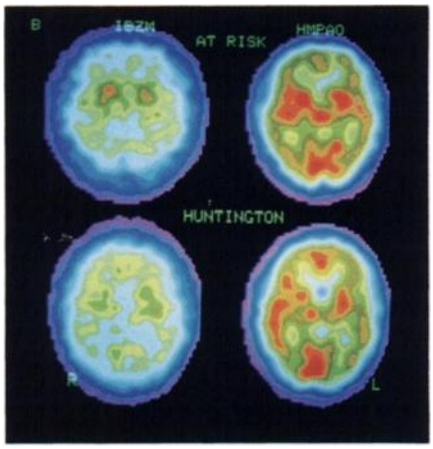

FIGURE 4. (A) Transaxial IBZM and HMPAO images through the basal ganglia from a normal control subject (top) and an at-risk subject (bottom). Striatal IBZM and HMPAO activities in the at-risk subject are similar to those of the normal control subject. (B) Another at-risk subject (top) and a symptomatic HD patient (bottom). Striatal IBZM uptake in the at-risk subject is slightly decreased, whereas HMPAO uptake is normal. Striatal IBZM and HMPAO uptakes are both reduced in the symptomatic patient. All images have been scaled according to BG-to-FC ratios for intersubject visual comparison.

tor findings did not allow a clinical diagnosis of HD to be made in these subjects. In addition, neither these subjects nor the other at-risk subjects demonstrated chorea under stressed conditions, such as tandem walking, performing complex facial movements or rapid alternating movements.

When compared with previously published normal values (*9,36,37*), the FH-to-CC ratios of those who had CT scans (n = 8), including three symptomatic patients and five at-risk subjects, with two of the latter having decreased IBZM ratios, indicated no significant caudate atrophy.

Genetic risk calculation showed that 37% ± 11% or 7 ± 2 (mean ± 1 s.d.) individuals in our at-risk group would be expected to be carriers of the HD gene on probability grounds. The number of at-risk individuals with abnormal IBZM BG-to-FC ratios is thus at 1 s.d. below the mean value and the number with abnormal HMPAO BG-to-FC ratios is more than 2 s.d. below the mean value.

DISCUSSION

Previous PET studies using ^{11}C-raclopride, a radioligand that binds reversibly to D2 receptors, have shown that the ratio of the radioligand uptake in the striatum relative to cerebellum under secular equilibrium conditions is independent of blood flow and provides an index of B_{max}/K_d (*40*). The dissociation constant, K_d, appears to be unaffected by age or disease states (*3,41,42*). This ratio thus reflects the maximal density of D2 binding sites in the striatum (B_{max}).

IBZM is also a D2 receptor ligand with high affinity and specificity and is chemically a close analog of raclopride (*25*). Thus, IBZM dissociates rapidly from receptors, allowing binding equilibrium to be established within a practical time span for SPECT scanning. Measurements can be made by obtaining a single SPECT scan during this "equilibrium phase" (*26,32*). In this study, the frontal cortex rather than the cerebellum was used as a reference region since the former has been recently suggested to be a more reliable reference than the latter (*26,43*). Our mean normal control IBZM BG-to-FC ratio is comparable to those reported by others (*26,27,44*). Slight differences are likely related to factors such as mean age, system resolution, attenuation correction method, choice of reconstruction filter and region size (*27*). To reduce statistical sampling errors, our striatal ROI was roughly 2 × $(FWHM)^3$ in volume. The use of a multiheaded SPECT system with higher system resolution should provide higher BG-to-FC ratios by permitting a smaller striatal region size. Tatsch et al. (*27*), however, reported that lower BG-to-FC ratios obtained without attenuation correction were comparable to higher values obtained with attenuation correction in discriminating between different patient groups. BG-to-FC ratios obtained under identical imaging conditions in the absence of striatal atrophy thus allow semiquantitative comparisons of D2 receptor status between subjects.

The decline in D2 receptor binding by 1.5% per decade is consistent with previous IBZM-SPECT findings (*26*) and also agrees with the 2.2% decline per decade found in the

TABLE 3
Summary of Neurological Examination

Clinical diagnosis (age)	Duration (mo)	S&F*	M&Q†	MMS‡
HD (68)§	24	8	10	23
HD (28)¶	24	10	4	28
HD (43)¶	12	11	6	26
HD (42)¶	12	10	4	28
At risk (40)¶	0	13	2	28
At risk (29)§	0	13	2	30
At risk (42)§	0	13	1	30
At risk (38)	0	13	1	30
At risk (17–64)** [n = 16]	0	13	0	30

*S&F: Functional capacity scale of Shoulson and Fahn (normal = 13, most severe = 0).

†M&Q: Marsden and Quinn's chorea scale (normal = 0, most severe = 24). At risk subjects with the M&Q scores of 1 and 2 had nonchoreic motor abnormalities characterized by occasional facial and/or limb "twitches."

‡MMS: Mini-mental state examination (normal = 30, most severe = 0).

§Only IBZM ratios are decreased in these subjects.

¶Both IBZM and HMPAO ratios decreased in these subjects.

**Included are one subject with both decreased IBZM and HMPAO ratios and another subject with a decreased IBZM ratio only.

TABLE 4
Summary of SPECT Imaging and Neurological Findings in At-Risk Subjects (n = 20)

No. of subjects	SPECT imaging		Neurological
	IBZM	HMPAO	
1	+	+	+*
1	+	+	–
2	+	–	+*
1	+	–	–
1	–	–	+*
14	–	–	–
Total positives	5	2	4

Abnormal test is indicated by a positive sign and normal test by a negative sign.

*+: Subtle nonchoreic motor abnormalities with or without slight abnormalities on the Mini-mental state test. For further description, see text.

postmortem study of Seeman et al. (*45*). Wong et al., however, found an apparent decline of 20% in the third decade of life in NMSP binding (*44*). Seeman et al. (*45*) suggested that the difference between their findings and those of Wong et al. might be related to the effect of a less permeable blood-brain barrier with aging because measurements with NMSP were made when less than 50% equilibrium had occurred (*46*) and that a more rapidly equilibrating radioligand such as raclopride (and hence IBZM) might be indicated for in vivo measurement of D2 receptor densities.

Our findings of decreased BG-to-FC IBZM ratios in all symptomatic HD patients are similar to those of Brücke et al. (*26*) who suggested that this is due to the loss of striatal D2 receptors. This may be partly explained, however, by a reduction in available binding sites due to competing endogenous dopamine since striatal concentrations of dopamine may be increased in HD (*4,6*). The effects of endogenous dopamine on raclopride binding were demonstrated previously (*43,47,48*) and similar results have been recently obtained for IBZM in nonhuman primates (*49*).

In this study, decreased IBZM BG-to-FC ratios were also seen in at-risk subjects, thus providing evidence that D2 receptor density and/or availability may be reduced during the asymptomatic stage. This finding provides a basis for subclinical dopaminergic dysfunction elicited by administering L-dopa in some at-risk subjects (*21*). The fact that subtle involuntary motor abnormalities, albeit nonchoreic, were detectable in some of our at-risk subjects with decreased IBZM ratios further supports this hypothesis. Thus, IBZM-SPECT may be useful for preclinical detection in asymptomatic at-risk subjects as well as confirming the diagnosis of HD in early symptomatic patients.

Both a reduction in striatal D2 receptor density and striatal hypoperfusion or hypometabolism, however, may be also found in other movement disorders, such as progressive supranuclear palsy, neuroacanthocytosis, Wilson's disease, multiple system atrophy, etcetera (*19,20,50*). Thus, none of the metabolic, perfusion or D2 receptor findings are specific for HD.

More recent evidence suggests that dopamine differentially regulates the two parallel major output pathways from the striatum which exert opposing effects upon the thalamus, including the "direct" pathway via postsynaptic D1 receptors and the "indirect" pathway via postsynaptic D2 receptors (*51–53*). It also has been shown that the decline in the influence of this "indirect" pathway in primates results in the development of chorea by releasing thalamic inhibition (*54,55*) and that there is a selective loss of D2 receptor-associated neurons in the striatum in the early stage of HD (*56*).

In the later stage of HD, bradykinesia and akinesia develop. This was shown to result from interference with the "direct" pathway due to the additional loss of D1 receptor-associated neurons in the striatum which would lead to increased thalamic inhibition (*57*). In fact, this would explain the apparent paradox of the coexistence of chorea and bradykinesia in advanced HD (*58*). Thus, the striatal D2 receptor deficit seen in HD patients might be more specific for chorea than perfusion or metabolism abnormalities, which simply represent diminished neuronal function (*22,59*) whether they are of D1 or D2 receptor cell types.

With the nigrostriatal system intact in HD (*4–6,22*), the striatal D2 receptor deficit appears to be the major factor for selective underactivity of the "indirect" pathway which is responsible for chorea. There is, however, some evidence suggesting that the striatal acetylcholinergic system selectively inputs into this "indirect" pathway and that it may mediate antagonistic effects to those of dopamine (*60*). This cholinergic system appears relatively spared in early HD (*6*).

The importance of dopaminergic-cholinergic balance for normal striatal function has been postulated previously (*1*). Perhaps our at-risk subjects with a decreased striatal IBZM ratio did not present chorea because they were maintaining a delicate balance of this system despite the reduction in D2 receptor density. However, the dopaminergic-cholinergic system of those at-risk subjects with both decreased IBZM ratios and subtle involuntary motor abnormalities may be in a more delicate balance. A further decline in D2 density might result in the development of chorea by disturbing this balance. The degree of D2 receptor density deficit associated with chorea may also depend on the subject's age in view of the age-dependence factor for the D2 receptor density. To confirm this and also to learn whether those at-risk subjects with abnormal SPECT studies will eventually develop HD, longitudinal follow-up studies are warranted.

Our semiquantitative analysis of striatal perfusion using HMPAO-SPECT indicates that this technique is less sensitive than IBZM-SPECT in detecting striatal abnormalities in both early symptomatic and at-risk subjects. Among our three semiquantitative HMPAO indices, the HMPAO BG-to-FC ratio was most consistently abnormal. However, if frontal cortical perfusion was decreased, as might be the case in patients with advanced HD, this ratio may be falsely elevated. In this study, such a false elevation was

unlikely since frontal perfusion as estimated by the HMPAO FC-to-CE ratio was normal in both symptomatic and at-risk groups. Although several other quantitative methods to evaluate striatal perfusion with SPECT have been described (*15,61,62*), there is no standard method (*19*).

Somewhat discrepant striatal metabolic findings among PET studies in at-risk subjects have been reported and these may be related to differing methodologies and/or biological factors such as age (*63,64*). None of the neurological criteria included chorea in the definition of "at-risk." The differences in the criteria used, however, might have contributed to the variation in subtle neurological findings between studies (*65*). We used neurological criteria adopted by Hayden et al. (*17*), and the fact that we could detect subtle, nonchoreic neurological signs in some at-risk subjects is consistent with their results as well as those of Mazziotta and Grafton et al. who used yet another scoring system to grade motor abnormalities (*16,65*).

In their PET study, Mazziotta et al. (*16*) reported decreased caudate glucose metabolism in 31% of their at-risk group. In terms of the estimated percentage of gene carriers and average age, their group (34%, 34.8 yr) was similar to ours (37%, 31.4 yr). HMPAO-SPECT may then be a less sensitive technique than PET in detecting striatal hypofunction in these subjects. However, IBZM-SPECT detected striatal abnormalities in a significantly higher percentage of our at-risk subjects (25%), which is within the percentage range of HD gene carriers on probabilistic grounds and is only slightly less than that of the at-risk subjects showing striatal hypometabolism in the study of Mazziotta et al. (*16*). IBZM-SPECT thus may be as sensitive as metabolic PET studies in detecting striatal abnormalities in at-risk subjects. To confirm this, comparative studies between SPECT and PET techniques in the same individuals are needed.

Finally, predictive testing of HD carriers may be done by identification of the DNA-linked polymorphic marker for HD (*66*). This test could have been optimally utilized in this study. However, this was not performed in view of the fact that the crucial family members of our at-risk subjects were not available because they either are living abroad or have deceased. In fact, the lack of an adequate family structure is a serious limitation in predictive DNA testing for HD (*67*). In addition, predictive DNA analysis has other limitations, including a recombination error of approximately 4% (*66*) and an error of up to 10% due to nonheterogeneity of the marker site (*68*). Until the HD gene can be directly identified, the use of this test as a gold standard should be viewed cautiously (*65*). IBZM D2 receptor SPECT imaging is thus a promising and potentially important practical alternative diagnostic tool that permits investigation of individuals at risk for HD.

ACKNOWLEDGMENTS

The authors thank Dr. Hank F. Kung, Department of Radiology, University of Pennsylvania, for providing the precursor BZM; Nordion International Inc., Vancouver for supplying part of the sodium ^{123}I-iodide; Amersham Canada Inc. for supplying HMPAO (Ceretec); Elscint Canada for financial support; Douglass C. Vines, RTNM and Bernardita Aguirre, MD for technical support; and Dae-Gyun Chung, MD, PhD and Bruce Gray, MD for valuable suggestions. Preliminary work for this study was presented at the 39th Annual Meeting of the Society of Nuclear Medicine, Los Angeles, CA, June 1992.

REFERENCES

1. Martin JB. Huntington's disease: new approaches to an old problem. *Neurology* 1984;34:1059–1072.
2. Vonsattel JP, Myers RH, Stevens TJ, et al. Neuropathological classification of Huntington's disease. *J Neuropath Exp Neurol* 1985;44:559–577.
3. Reisine TD, Fields JZ, Bird ED, Spokes E. Characterization of brain dopamine receptors in Huntington's disease. *Commun Psychopharmacol* 1978;2:79–84.
4. Spokes EGS. Neurochemical alterations in Huntington's chorea. *Brain* 1980;103:179–210.
5. Whitehouse PJ, Trifiletti RR, Jones BE, et al. Neurotransmitter receptor alterations in Huntington's disease. *Am J Neurol* 1985;18:202–210.
6. Bird ED, Iversen LL. Huntington's chorea. Post-mortem measurement of glutamic acid decarboxylase, choline acetyltransferase, and dopamine in basal ganglia. *Brain* 1974;97:452–472.
7. Cross A, Rossor M. Dopamine D1 and D2 dopamine receptors in Huntington's disease. *Eur J Pharmacol* 1983;88:223–229.
8. Conneally PM. Huntington's disease: genetics and epidemiology. *Am J Hum Genet* 1984;36:506–526.
9. Terrence CF, Delaney JF, Alberts MC. Computed tomography for Huntington's disease. *Neuroradiology* 1977;13:173–175.
10. Simmons JT, Pastakia B, Chase TN, et al. Magnetic resonance imaging in Huntington's disease. *Am J Neuroradiol* 1986;7:25–28.
11. Kuhl DE, Phelps ME, Markham CH, et al. Cerebral metabolism and atrophy in Huntington's disease determined by F-18 DG and computed tomographic scan. *Ann Neurol* 1982;12:325–434.
12. Hayden MR, Martin WRW, Stoessl AJ, et al. Positron emission tomography in the early diagnosis of Huntington's disease. *Neurology* 1986;36:888–894.
13. Reid IC, Besson JAO, Best PV, et al. Imaging of cerebral flow markers in Huntington's disease using single photon emission computed tomography. *J Neurol Neurosurg Psychiatry* 1988;51:1264–1268.
14. Smith FW, Gemmell HG, Sharp PF, et al. Technetium-99m HMPAO imaging in patients with basal ganglia disease. *Br J Radiol* 1988;61:914–920.
15. Leblhuber F, Hoell K, Reisecker F, et al. Single photon emission computed tomography in Huntington's chorea. *Psychiatry Res* 1989;29:337–339.
16. Mazziotta JC, Phelps ME, Pahl JJ, et al. Reduced cerebral glucose metabolism in persons at risk for Huntington's disease. *N Engl J Med* 1987;316:357–362.
17. Hayden MR, Hewitt J, Stoessl AJ, Clark C, Ammann W, Martin WRW. The combined use of positron emission tomography and DNA polymorphism for preclinical detection of Huntington's disease. *Neurology* 1987;37:1441–1447.
18. Finch CE. The relationship of aging changes in the basal ganglia to manifestation of Huntington's chorea. *Ann Neurol* 1980;7:406–411.
19. Nagel JS, Ichise M, Holman BL. The scintigraphic evaluation of Huntington's disease and other movement disorders using single photon emission computed tomography perfusion brain scans. *Semin Nucl Med* 1991;21:11–23.
20. Alavi A, Hirsch LJ. Studies of central nervous system disorders with single photon emission computed tomography and positron emission tomography: evolution over the past two decades. *Semin Nucl Med* 1991;21:58–81.
21. Klawans HL, Paulson GW, Ringel SP, Barbeau A. Use of L-dopa in the detection of presymptomatic Huntington's chorea. *N Engl J Med* 1972;286:1331–1334.
22. Leenders KL, Frackowiak RSJ, Quinn N, Marsden CD. Brain energy metabolism and dopaminergic function in Huntington's disease measured in vivo using positron emission tomography. *Mov Dis* 1986;1:69–77.
23. Hagglund J, Aquilonius SM, Eckernas SA, et al. Dopamine receptor properties in Parkinson's disease and Huntington's chorea evaluated by positron emission tomography using ^{11}C-methyl-spiperone. *Acta Neurol Scand* 1987;75:87–94.
24. Alavi A, Velchik MG, Kung HF, et al. Imaging of the basal ganglia in the

human brain with I-123-IBZM: a new CNS D2 receptor agent [Abstract]. *J Nucl Med* 1989;30:731.
25. Kung HF, Alavi A, Chang W, et al. In vivo SPECT imaging of CNS D-2 dopamine receptors: initial studies with iodine-123-IBZM in humans. *J Nucl Med* 1990;31:573–579.
26. Brücke T, Podreka I, Angelberger P, et al. Dopamine D2 receptor imaging with SPECT: studies in different neuropsychiatric disorders. *J Cereb Blood Flow Metab* 1991;11:220–228.
27. Tatsch K, Schwarz J, Oertel WH, Kirsch C-M. SPECT imaging of dopamine D2 receptors with ^{123}I-IBZM: initial experience in controls and patients with Parkinson's syndrome and Wilson's disease. *Nucl Med Commun* 1991; 12:699–707.
28. Shoulson I, Fahn S. Huntington's disease: clinical care and evaluation. *Neurology* 1979;29:1–3.
29. Marsden CM, Quinn N. Appendix 6. In: Lader MH, Richen A, eds. *Methods in clinical pharmacology of the nervous system*. London: MacMillan; 1981:103.
30. Folstien ME, Folstien SE, McHugh PR. Minimental state: a practical method for grading the cognitive state of patients for the clinician. *J Psychiatr Res* 1975;12:189–198.
31. Kung M-P, Liu B-L, Yang Y-Y, Billings JJ, Kung HF. A kit formulation for preparation of iodine-123-IBZM: a new CNS D-2 dopamine receptor imaging agent. *J Nucl Med* 1991;32:339–342.
32. Toyama H, Ichise M, Ballinger JR, Fornazzari L, Kirsh JC. Dopamine D_2 receptor imaging: basic in vivo characteristics and clinical applications of ^{123}I-IBZM in humans. *Ann Nucl Med* 1993;7:29–38.
33. Chang L-T. A method for attenuation correction in radionuclide computed tomography. *IEEE Trans Nucl Sci* 1978;NS-25:638–643.
34. Ichise M, Toyama H, Vines DC, Chung D-G, Kirsh JC. Neuroanatomical localization for clinical SPECT perfusion brain imaging: a practical proportional grid method. *Nucl Med Commun* 1992;13:861–866.
35. Talairach J, Tournoux P, Rayport M, eds. *Co-planar stereotaxic atlas of the human brain. 3-dimensional proportional system: an approach to cerebral imaging*. New York: Thieme Inc.; 1988:1–122.
36. Neophyteides AN, DiChiro G, Baron SA, Chase TN. Computed axial tomography in Huntington's disease and persons at risk for Huntington's disease. *Adv Neurol* 1979;23:185–191.
37. Barr AN, Heinze WJ, Dobben GD, Valvassori GE, Sugar O. Bicaudate index in computerized tomography of Huntington's disease and cerebral atrophy. *Neurology* 1978;28:1196–1200.
38. Pericak-Vance MA, Elston RC, Conneally PM, et al. Age-of-onset heterogeneity in Huntington's disease families. *Am J Genet* 1983;14:49–59.
39. Shoulson I. Huntington's disease: functional capacities in patients treated with neuroleptic and antidepressant drugs. *Neurology* 1981;31:1333–1335.
40. Farde L, Hall H, Ehrin E, et al. Quantitative analysis of D2 dopamine receptor binding in living human brain by PET. *Science* 1986;231:258–261.
41. Morgan DG, Marcusson JA, Nyberg P, et al. Divergent changes in D-1 and D-2 dopamine binding sites in human brain during aging. *Neurobiol Aging* 1987;8:195–201.
42. Guttman M, Seeman P. Dopamine D2 receptor density in Parkinsonian brain is constant for duration of disease, age, and duration of L-dopa therapy. *Adv Neurol* 1986;45:51–57.
43. Seeman P, Niznik HB, Guan H-C. Elevation of dopamine D_2 receptors in schizophrenia is underestimated by radioactive raclopride [Letter]. *Arch Gen Psychiatry* 1990;47:1170–1172.
44. Costa DC, Verhoeff NPLG, Cullum PJ, et al. In vivo characterisation of 3-iodo-6-methoxybenzamide ^{123}I in humans. *Eur J Nucl Med* 1990;16:813–816.
45. Seeman P, Bzowej NH, Guan H-C, et al. Human brain dopamine receptors in children and aging adults. *Synapse* 1987;1:399–404.
46. Wong DF, Wagner HN, Dannals RJ, et al. Effects of age on dopamine and serotonin receptors measured by positron tomography in the human brain. *Science* 1984;226:1393–1396.
47. Seeman P, Guan H-C, Niznik HB. Endogenous dopamine lowers the D2 receptor density as measured by ^{3}H-raclopride: implications for positron emission tomography of the human brain. *Synapse* 1989;3:96–97.
48. Young LT, Wong DF, Goldman S, et al. Effects of endogenous dopamine on kinetics of [^{3}H]N-methylspiperone and [^{3}H]raclopride binding in the rat brain. *Synapse* 1991;9:188–194.
49. Innis RR, Mallison RT, Al-Tikriti M, et al. Amphetamine-stimulated dopamine release competes in vivo for [^{123}I]IBZM binding to the D2 receptor in nonhuman primates. *Synapse* 1992;10:177–184.
50. Playford ED, Brooks DJ. In vivo and in vitro studies of the doperminergic system in movement disorders. *Cerebreovasc Brain Metab Rev* 1992;4:144–171.
51. Gerfen CR, Engber TM, Mahan LC, et al. D1 and D2 dopamine receptor-regulated gene expression of striatonigral and striatopallidal neurons. *Science* 1990;250:1429–1432.
52. Albin RL, Young AB, Penney JB. The functional anatomy of basal ganglia disorders. *Trends Neurosci* 1989;12:366–375.
53. Alexander GE, Crutcher MD. Functional architecture of basal ganglia circuits: neural substrates of parallel processing. *Trends Neurosci* 1990;13: 266–271.
54. Delong MR. Primate models of movement disorders of basal ganglia origin. *Trends Neurosci* 1990;13:281–285.
55. Mitchell IJ, Jackson A, Sambrook MA, Crossman AR. The role of the subthalamic nucleus in experimental chorea. *Brain* 1989;112:1533–1548.
56. Reiner A, Albin RL, Anderson KD, D'Amato CJ, Penney JB, Young AB. Differential loss of striatal projection neurons in Huntington disease. *Proc Natl Acad Sci USA* 1988;85:5733–5737.
57. Albin RL, Reiner A, Anderson KD, Penney JB, Young AB. Striatal and nigral neuron subpopulations in Huntington's disease: implications for the functional anatomy of chorea and rigidity-akinesia. *Ann Neurol* 1990;13: 266–271.
58. Thompson PD, Beradelli A, Rothwell JC, et al. The coexistence of bradykinesia and chorea in Huntington's disease and its implications for theories of basal ganglia control of movement. *Brain* 1988;111:223–244.
59. Sokolof L. The relationship between function and energy metabolism: its use in the localization of functional activity in the nervous system. *Neurosci Res Prog Bull* 1981;19:159–210.
60. Scheel-Kruger J. New aspects on the functional role of acetylcholine in the basal ganglia system: interactions with other neurotransmitters. In: Singh MM, Lal H, eds. *Central cholinergic mechanisms of adaptive dysfunctions*. New York: Plenum Press; 1985:105–139.
61. Nagel JS, Johnson KA, Ichise M, et al. Decreased iodine-123 IMP caudate nucleus uptake in patients with Huntington's disease. *Clin Nucl Med* 1988; 13:486–490.
62. Podreka I, Suess E, Goldenberg G, et al. Initial experience with technetium-99m-HM-PAO brain SPECT. *J Nucl Med* 1987;28:1657–1666.
63. Hayden MR, Hewitt J, Martin WRW, Clark C, Ammann W. Studies in persons at risk for Huntington's disease [Letter]. *N Engl J Med* 1987;317: 382–383.
64. Mazziotta JC, Phelps ME, Pahl JJ, et al. Studies in persons at risk for Huntington's disease [Letter]. *N Engl J Med* 1987;317:383–384.
65. Grafton ST, Mazziotta JC, Pahl JJ, et al. A comparison of neurological, metabolic, structural, and genetic evaluations in persons at risk for Huntington's disease. *Ann Neurol* 1990;28:614–621.
66. Gusella JF, Wexler NS, Conneally PM, et al. A polymorphic DNA marker genetically linked to Huntington's disease. *Nature* 1983;306:234–238.
67. Harper PS, Sarfarazi M. Genetic prediction and family structure in Huntington's chorea. *Br Med J* 1985;290:129–131.
68. Gusella JF, Tanzi RE, Bader PJ, et al. Deletion of Huntington's disease linked G8(D4S10) locus in Wolf-Hirschorn syndrome. *Nature* 1985;318:75–78.